

ON THE NATURE OF SEYFERT GALAXIES WITH HIGH [OIII]5007 BLUESHIFTS

S. KOMOSSA

Max-Planck-Institut für extraterrestrische Physik, Giessenbachstrasse 1, 85748 Garching, Germany; skomossa@mpe.mpg.de

D. XU

National Astronomical Observatories, Chinese Academy of Science, A20 Datun Road, Chaoyang District, Beijing 100012, China

H. ZHOU

Max-Planck-Institut für extraterrestrische Physik, Giessenbachstrasse 1, 85748 Garching, Germany

T. STORCHI-BERGMANN

Instituto de Fisica, UFRGS, Campus do Vale, CP 15051, Porto Alegre 91501-970, RS, Brazil

AND

L. BINETTE

Département de Physique, de Génie Physique et d'Optique, Université Laval, Québec, QC, G1K7P4, Canada; and Instituto de Astronomía, UNAM, Ap. 70-264, 04510 México, DF, México

Draft version October 25, 2018

ABSTRACT

We have studied the properties of Seyfert galaxies with high [OIII]5007 blueshifts (“blue outliers”), originally identified because of their strong deviation from the $M_{\text{BH}} - \sigma$ relation of normal, narrow-line Seyfert 1 (NLS1) and broad-line Seyfert 1 (BLS1) galaxies. These blue outliers turn out to be important test-beds for models of the narrow-line region (NLR), for mechanisms of driving large-scale outflows, for links between NLS1 galaxies and radio galaxies, and for orientation-dependent NLS1 models. We report the detection of a strong correlation of line blueshift with ionization potential in each galaxy, including the measurement of coronal lines with radial velocities up to 500–1000 km s⁻¹, and we confirm a strong correlation between [OIII] blueshift and line width. All [OIII] blue outliers have narrow widths of their broad Balmer lines and high Eddington ratios. While the presence of non-shifted low-ionization lines signifies the presence of a classical outer quiescent NLR in blue outliers, we also report the absence of any second, non-blueshifted [OIII] component from a classical inner NLR. These results place tight constraints on NLR models. We favor a scenario in which the NLR clouds are entrained in a decelerating wind which explains the strong stratification and the absence of a zero-blueshift inner NLR of blue outliers. The origin of the wind remains speculative at this time (collimated radio plasma, thermal winds, radiatively accelerated clouds). It is perhaps linked to the high Eddington ratios of blue outliers. Similar, less powerful winds could be present in all Seyfert galaxies, but would generally only affect the coronal line region (CLR), or level off even before reaching the CLR. Similarities between blue outliers in NLS1 galaxies and (compact) radio sources are briefly discussed.

Subject headings: galaxies: active – galaxies: evolution – galaxies: individual (SBS0919+515, SDSSJ115533.50+010730.4, RXJ01354-0043, NGC450#86, SDSSJ032606.75+011429.9, IRAS11598-0112, SDSSJ171828.99+573422.3, PG1244+026, RXJ09132+3658) – galaxies: Seyfert – quasars: emission lines

1. INTRODUCTION

The concept of feedback due to outflows is a potential key ingredient in understanding the coevolution of galaxies and black holes (Silk & Rees 1998, Fabian 1999, Wyithe & Loeb 2003). Recent analytic estimates and simulations demonstrate the importance of feedback from winds/outflows for instance in cosmic downsizing (Scannapieco et al. 2005), in fixing the $M_{\text{BH}} - \sigma$ relation (di Matteo et al. 2005), and in determining galaxy colors (Springel et al. 2005) by regulating star formation in the host galaxy. Powerful gaseous outflows in Active Galactic Nuclei (AGN) deposit mass, energy and metals in the interstellar medium of the galaxy and the inter-

galactic medium or intracluster medium (Colbert et al. 1996, Churazov et al. 2001, Moll et al. 2007). AGN winds also play a potentially important role in unified models of AGN (Elvis 2000, 2006).

Observational evidence for outflows in AGN exists on various scales and in all wavebands from the radio (Morganti et al. 2005, Gallimore et al. 2006), to the IR (Rodríguez-Ardila et al. 2006), optical (Das et al. 2005), UV (Sulentic et al. 2007, Rodríguez Hidalgo et al. 2007, Crenshaw & Kraemer 2007), and X-ray band (Chelouche & Netzer 2005, Krongold et al. 2007); see Veilleux et al. (2005) for a review. There are several lines of evidence that outflows are particularly strong in narrow-line Seyfert 1 (NLS1) galaxies. NLS1 galaxies are a subclass

of AGN with extreme emission-line and continuum properties which appear to be in part driven by their high Eddington ratios, low black hole masses, and other parameters (e.g., Osterbrock & Pogge 1985, Boroson 2002, Grupe 2004; see Komossa 2008 for a review). The high Eddington ratios likely lead to strong, radiation-pressure driven outflows.

As a class of objects with low black hole masses, high accretion rates and strong winds, the location of NLS1 galaxies on the $M_{\text{BH}} - \sigma$ plane is of special interest (Mathur et al. 2001; see our Sect. 4.1). Komossa & Xu (2007) have shown that NLS1 galaxies follow the same $M_{\text{BH}} - \sigma$ relation as normal and broad-line Seyfert 1 (BLS1) galaxies, if the width of the [SII]6716,6731 emission lines is used as a surrogate for stellar velocity dispersion. The width of [OIII]5007 (after removal of asymmetric blue wings) is still a good proxy for stellar velocity dispersion in BLS1 and NLS1 galaxies, with one important exception. A subset of NLS1 galaxies deviates systematically from the $M_{\text{BH}} - \sigma$ relation, and all of these are characterized by high [OIII] blueshifts. At the same time, the [SII]-based measurements of velocity dispersion of the same objects still place them on the $M_{\text{BH}} - \sigma$ relation (Fig. 1). Therefore, the [OIII] lines of these particular galaxies were not suitable to estimate σ . However, the independent question is raised as to which mechanism drives these [OIII] line blueshifts, and what we can learn from them regarding the nature of these systems and perhaps the evolutionary state of NLS1 galaxies. That is the topic of this study.

A measurable difference in blueshifts and widths of different NLR emission lines has been recognized early (review by Osterbrock 1991). The phenomenon of strong [OIII] blueshifts exceeding one–several hundred km s^{-1} (so-called blue outliers), is more rare. It has been detected early in individual objects (Phillips 1976) but has only been studied systematically recently (Zamanov et al. 2002, Marziani et al. 2003, Aoki et al. 2005, Boroson 2005, Bian et al. 2005). These studies have shown that blue outliers have high Eddington ratios and small Balmer line widths (all of them with $\text{FWHM}(\text{H}\beta) < 4000 \text{ km s}^{-1}$, and most of them with $\text{FWHM}(\text{H}\beta) < 2000 \text{ km s}^{-1}$; Marziani et al. 2003). It has remained uncertain whether there is (Bian et al. 2005) or is not (Aoki et al. 2005) a direct correlation between [OIII] blueshift and Eddington ratio. Common to most studies is the presence of a strong correlation between [OIII] blueshift and [OIII] line width. This correlation is also known among iron coronal lines of BLS1 galaxies (Penston et al. 1984, Erkens et al. 1997). The reason is not yet well understood. Outflows are thought to play a role in explaining the phenomenon.

Except Boroson (2005) all sample studies concentrated on the [OIII]- $\text{H}\beta$ region of optical spectra of blue outliers in order to examine the phenomenon, while for the first time we include information from all the detected optical NLR lines. We report the detection of strong correlations and discuss consequences for the nature of blue outliers and for dynamical NLR models. This paper is organized as follows. In Sect. 2 we describe the sample selection and provide details on the data analysis. Results on trends and correlations are presented in Sect. 3 which are then discussed in Sect. 4. A sum-

mary and conclusions are given in Sect. 5. Some individual objects turn out to be remarkable. Notes on them are provided in an Appendix. We use a cosmology with $H_0=70 \text{ km s}^{-1} \text{ Mpc}^{-1}$, $\Omega_{\text{M}}=0.3$ and $\Omega_{\Lambda}=0.7$ throughout this paper.

2. DATA ANALYSIS

2.1. The sample

The nine NLS1 galaxies of the present work were drawn from the sample of Xu et al. (2007, 2008). The original sample selection and standard data reduction procedures were described in detail in that work. In brief, the sample consists of NLS1 galaxies from the catalogue of Véron-Cetty & Véron (2003) and a comparison sample of BLS1 galaxies from Boroson (2003) at redshift $z < 0.3$, which have Sloan Digital Sky Survey (SDSS) DR3 (Abazajian et al. 2005) spectra available and which have detectable low-ionization lines (presence of [SII]6716,6731, with $\text{S/N} > 5$). The BLS1 and NLS1 galaxy samples have similar redshift and absolute magnitude distributions. Xu et al. (2007) corrected the SDSS spectra for Galactic extinction, decomposed the continuum into host galaxy and AGN components, and then subtracted the host galaxy contribution and the FeII complexes from the spectra. Emission line profiles of the galaxies were fit with Gaussians using the IRAF package SPECFIT (Kriss 1994). Measured FWHMs were corrected for instrumental broadening. Re-classification after spectral emission-line fitting led to 39 BLS1 and 55 NLS1 galaxies in the sample. We focus here on the nine galaxies with the highest blueshifts of [OIII] (Tab. 1) which were identified by Komossa & Xu (2007; KX07 hereafter). Results from the complete NLS1 (and BLS1) sample are shown for comparison purposes, and in order to identify trends across the whole BLS1 – NLS1 – blue-outlier population. When we report measurements of optical FeII strength (FeII4570), this is the integrated flux of the FeII emission complex between the rest wavelengths 4434Å and 4684Å. We refer to the flux sum of the two Sulphur lines, [SII]6716 and [SII]6731, as [SII]6725.

2.2. Emission-line fits and [OIII] profile

The Balmer lines were decomposed into three components, narrow core ($\text{H}\beta_{\text{n}}$; FWHM fixed to that determined for [SII]6716,6731), and two broad components. No physical meaning is ascribed to the two separate broad components; they merely serve as a mathematical description (see Xu et al. 2008 for alternative Lorentzian fits). The final width of the broad-line emission, $\text{H}\beta_{\text{b}}$, is determined as the FWHM of the sum of the two Gaussians. With the exception of [OIII], forbidden lines are well represented by single Gauss profiles. The total [OIII] emission-line profile, $[\text{OIII}]_{\text{tot1}}$, was decomposed into two Gaussian components, a narrow core ($[\text{OIII}]_{\text{c}}$) and broad base. We distinguish between two types of [OIII] spectral complexity: (1) the presence of such a broad base which tends to be blue-asymmetric (e.g., Heckman et al. 1981), and is referred to as “blue wing”, and (2) systematic blueshifts of the whole core of [OIII]. Objects which show this latter phenomenon are called “blue outliers” (Zamanov et al. 2002)¹. Measurements of the FWHM

¹ Note that we use a velocity shift of $v_{[\text{OIII}]_{\text{c}}} > 150 \text{ km s}^{-1}$ in order to refer to an object as [OIII] blue outlier; while Zamanov

and blueshift of [OIII] reported in this work refer to the core of the emission-line, unless noted otherwise.

Ideally, measurements of the velocity shift of [OIII] should be done relative to the galaxy restframe, as defined by stellar absorption lines from the host galaxy. However, these features are generally weak or absent in our galaxies (and in NLS1 galaxies in general). We therefore measure velocity shifts of [OIII] and of all other lines relative to [SII]. We use positive velocity values to refer to blueshifts, negative ones for redshift. The shifts of $H\beta$ and other low-ionization lines ([OI]6300, NII[6584], [OII]3727) agree well with [SII], while other high-ionization lines ([NeIII]3861, [NeV]3426, and iron coronal lines) are characterized by high blueshifts (Sect. 3.3). If lines were too faint to be fit by a Gaussian of free width, we used fixed width instead (fixed to $\text{FWHM}([\text{SII}])$ for low-ionization lines or to $\text{FWHM}([\text{OIII}]_c)$ for high-ionization lines) and determined the central wavelength to measure the blueshift. Results are reported in Tab. 1. Since the redshifts provided by the SDSS pipeline are determined based on all strong detected emission lines and are therefore influenced by the blueshifted [OIII], we have re-measured redshifts based on $H\beta_n$. It is these redshifts that are given in Tab. 1. We have measured the average $[\text{OIII}]_{\text{totl}}/[\text{SII}]6725$ ratios of our BLS1 and NLS1 galaxy sample. We find that, in terms of this ratio, their NLRs are similar, with $\langle [\text{OIII}]_{\text{totl}}/[\text{SII}]6725 \rangle = 5$ in BLS1 galaxies, and $\langle [\text{OIII}]_{\text{totl}}/[\text{SII}]6725 \rangle = 4$ in NLS1 galaxies.

Notes on individual objects are given in the Appendix. Here, we briefly comment on the detection of [FeX]6375 in two blue outliers. In PG1244+026 [FeX] is blended with [OI]6365. For decomposition, the width of [OI]6365 was fixed to that of [OI]6300. The two-component fit then reproduces the expected ratio of $[\text{OI}]6300/[\text{OI}]6365 \approx 3$. [FeX] is blueshifted by 640 km s^{-1} . In RXJ0135-0043, [FeX] overlaps with atmospheric O_2 which is imperfectly corrected for. Therefore, the width of [FeX] was fixed to that of [OIII]. This gives an outflow velocity of 990 km s^{-1} .

2.3. Robustness of spectral fits: continuum and line decomposition

In order to see how much the fitting procedure affects measurements of [OIII] fluxes, asymmetries and blueshifts, we have repeated the spectral analysis several times under different conditions and assumptions: We have fit the host-galaxy-corrected, FeII subtracted spectrum and for comparison the original SDSS spectrum without any of these corrections. We have re-fit the [OIII] profile in a number of different ways, and with different Gaussian decompositions. The [OIII] profile was fit using the red half of the profile only, or different fractions of the total profile, or only the upper 30% of the profile, or with a single and a double Gaussian profile. Fitting the profile with one single Gaussian component maximizes the blueshift in objects with significant [OIII] blue wings. In all other cases, uncertainties in line blueshifts due to non-subtraction of a host galaxy contribution and due to different line fitting procedures are typically much less than 50 km s^{-1} . The

blueshift independently determined from the weaker line [OIII]4959 also agrees with [OIII]5007 within better than 50 km s^{-1} . Four of our galaxies are also in the sample of Boroson (2005). His [OIII] blueshift measurements agree with ours within typically better than $\pm 10 \text{ km s}^{-1}$. Uncertainties in FWHM of the core of [OIII] are typically 30% for [OIII] lines with extra blue wing (smaller in others), and are due to uncertainties in decomposition. We note in passing that the frequency of [OIII] blue wings in blue outliers is neither particularly high nor low (see also Boroson 2005).

3. RESULTS

3.1. Constraints on the presence/absence of blueshifted emission lines

In order to facilitate a systematic discussion of NLR models of blue outliers (Sect. 4.3), we have investigated whether the non-shifted low-ionization lines have a (faint) high-ionization [OIII] counterpart and vice versa². We did this representatively for the three galaxies with the highest [OIII] blueshifts (SBS0919+515, SDSSJ11555+0107 and RXJ01354-0043), and for the galaxy with the highest S/N (PG1244+026). We have examined the following three questions:

(1) Is there any [OIII] emission at zero blueshift present in the spectrum (which could originate from the inner NLR; or be counterpart to the low-ionization emission lines from the outer NLR)? In order to test this, we have enforced an extra Gaussian line contribution to [OIII] at zero blueshift (or at $v_{[\text{OIII}]} = 50 \text{ km s}^{-1}$, the average value of our NLS1 sample excluding blue outliers) and of fixed $\text{FWHM}([\text{OIII}]_{\text{extra}}) = \text{FWHM}([\text{SII}])$. We find that, if present, it must be very weak. The average ratio $[\text{OIII}]_{\text{totl}}/[\text{SII}]6725$ in our BLS1 sample is 5, while in our NLS1 sample it is 4. This value of 4 is much higher than the upper limit on the extra component which was fit to the observed spectra: Typically, $[\text{OIII}]_{\text{extra}}/[\text{SII}]6725 \approx 0.1 - 0.4$, and always, $[\text{OIII}]_{\text{extra}}/[\text{SII}]6725 < 1$. Since the ratio of [OIII]/[SII] of nearby Seyfert galaxies generally decreases in dependence of radius (in models and observations; Komossa & Schulz 1997, Bennert et al. 2006) and since there must be an [OIII] contribution from the outer [SII] emitting clouds, the limits derived on any non-blueshifted [OIII] contribution from the *inner* NLR are very tight.

(2) Does the blueshifted [OIII] have a blueshifted $H\beta$ counterpart? I.e., how much highly blueshifted $H\beta$ could be 'hidden' in the $H\beta$ profile? In order to check this, we have re-fit $H\beta$ adding an additional Gaussian to describe its profile with parameters of this extra component fixed at $v_{H\beta_{\text{extra}}} = v_{[\text{OIII}]_c}$, $\text{FWHM}(H\beta_{\text{extra}}) = \text{FWHM}([\text{OIII}]_c)$ and an intensity ratio $[\text{OIII}]_c/H\beta_{\text{extra}} = 10$. We find that such a weak component could generally be hidden in the $H\beta$ profile.

(3) Does the blueshifted [OIII] have a blueshifted low-ionization counterpart in [SII]? This is not the case. For typical *spatially averaged* ratios of $[\text{OIII}]/[\text{SII}]6725 \approx 4$ of our NLS1 sample, blueshifted [SII] lines would have

² Note that, apart from [OIII], other high-ionization lines show blueshifts, too (Sect. 3.3.1), but they are too faint for multi-component line decompositions. Among the non-shifted emission lines, [SII] is the strongest unblended line, and we therefore focus on [SII] for the corresponding estimates in this section.

et al. (2002) use this terminology for objects with $v_{[\text{OIII}]} > 250 \text{ km s}^{-1}$, where [OIII] outflow velocity is measured relative to $H\beta$.

generally been detectable, but are absent. Very faint blueshifted [SII], as it may arise in the *inner* NLR, cannot be excluded with the present data.

In summary, we find (1) little evidence for zero-blueshift [OIII] emission (the amount of emission consistent with the spectra likely originates from the outer parts of the NLR which also emits in [SII] and other low-ionization lines); (2) an extra blueshifted component in $H\beta$ – the expected counterpart to blueshifted [OIII] – can be hidden in the $H\beta$ profile; and (3) there is no detectable highly blueshifted component in the low-ionization lines.

3.2. Estimates of black holes masses, Eddington ratios and NLR densities

Black hole masses were estimated by using the radius (R_{BLR})-luminosity (L) relation of BLS1 galaxies as reported by Kaspi et al. (2005) and the width of $H\beta$. The luminosities at 5100\AA were taken from Xu et al. (2008) and are based on SDSS g^* and r^* magnitudes corrected for Galactic extinction. Since we lack multi-wavelength spectral energy distributions, the bolometric luminosity L_{bol} was estimated using a standard bolometric correction of $L_{\text{bol}} = 9\lambda L_{5100}$ (Kaspi et al. 2000). L_{Edd} was calculated from the black hole mass, according to $L_{\text{Edd}} = 1.3 \cdot 10^{38} M_{\text{BH}}/M_{\odot}$ erg/s. Typical errors in individual BH mass estimates can be as large as 0.5 dex, and arise from the use of single-epoch data, and uncertainties in $H\beta$ decomposition and in host galaxy contribution. The NLR density was derived from the density-sensitive [SII] intensity ratio, [SII]6716/[SII]6731 (Xu et al. 2007).

3.3. Trends and correlations

We have checked for (1) trends of outflow velocity with other (atomic) parameters within each single spectrum, and (2) for trends across our sample of blue outliers (do all blue outliers have high Eddington ratios, high black hole masses, etc. ?), and (3) for trends across our whole sample of BLS1 and NLS1 galaxies.

3.3.1. A strong correlation of line shift with ionization potential

We detect a strong correlation between emission-line blueshift and ionization potential (Fig. 3). While the low-ionization forbidden lines of [OI], [OII] and [NII], and the Balmer lines $H\alpha$ and $H\beta$ are at velocities very similar to [SII], high-ionization lines on the other hand show strong blueshifts which increase with ionization potential. Two galaxies (SDSSJ115533.50+010730.4 and PG1244+026) show extreme blueshifts in [Fe X], on the order of $600\text{--}1000 \text{ km s}^{-1}$. There is also a correlation between outflow velocity and critical density of the individual line transitions (Fig. 3), but it is less tight in the sense that [OI]6300, which has low ionization potential but high critical density, does not follow the trend.

3.3.2. Trends and correlations of [OIII] blueshift with line and galaxy parameters

We have correlated the [OIII] blueshifts (of the blue outliers, and of our sample as a whole) with various other line parameters (line widths, line ratios) and with galaxy properties (absolute magnitude, black hole mass,

Eddington ratio, NLR density). The strongest correlation is the one between [OIII] blueshift and [OIII] line width (Spearman rank correlation coefficient $r_S=0.6$ for the whole NLS1 sample and even higher for just the blue outliers; Fig. 3). Within the NLS1 sample, there is a trend that blue outliers preferentially avoid low Eddington ratios L/L_{Edd} and low FeII/ $H\beta$ ratios. Most blue outliers have small ratios of [OIII]/ $H\beta_{\text{tot}}$. We do not find trends of outflow velocity with NLR density n_e , black hole mass, absolute magnitude M_i , and the width of the broad component of $H\beta$ (Fig. 4). However, while trends are absent within the NLS1 population itself, it is interesting to note that the presence of blue outliers amplifies trends which become apparent when the BLS1 galaxies are added to the correlation plots (Fig. 4).

3.4. Frequency of blue outliers

Among our sample, blue outliers only occur in NLS1 galaxies. At a velocity $v_{[\text{OIII}]} \gtrsim 150 \text{ km s}^{-1}$, we have a blue outlier fraction of 16%. If we use $v_{[\text{OIII}]} \gtrsim 250 \text{ km s}^{-1}$ instead, as in Zamanov et al. (2002), the fraction of blue outliers among NLS1 galaxies is 5%.

4. DISCUSSION

4.1. The locus of Seyfert galaxies with [OIII] blueshifts on the $M_{\text{BH}} - \sigma$ plane

Investigating the location of different types of galaxies on the $M_{\text{BH}} - \sigma$ plane, and their potential evolution across the plane, is of great interest in the context of galaxy formation and evolution models. In AGN, stellar velocity dispersion is often difficult to measure, and the width of [OIII] has become a convenient proxy for stellar velocity dispersion (e.g., Terlevich et al. 1990, Whittle 1992, Nelson & Whittle 1996, Nelson 2000, Shields et al. 2003, Boroson 2003, Greene & Ho 2005, Netzer and Trakhtenbrot 2007, Salviander et al. 2007) after removing [OIII] blue wings and excluding galaxies with powerful kiloparsec-scale linear radio sources. The scatter in the relation is larger than in the original $M_{\text{BH}} - \sigma_*$ relation (Ferrarese & Merritt 2000, Gebhardt et al. 2000), and indicates secondary influences on the gas kinematics (e.g., Nelson & Whittle 1996, Rice et al. 2006).

Mathur et al. (2001) pointed out the importance of studying the locus of NLS1 galaxies on the $M_{\text{BH}} - \sigma$ plane, which was the focus of a number of subsequent studies (Wang & Lu 2001, Wandel 2002, Botte et al. 2004, 2005, Bian et al. 2004, Grupe & Mathur 2004, Barth et al. 2005, Greene & Ho 2005, Mathur & Grupe 2005a,b, Zhou et al. 2006, Ryan et al. 2007, Watson et al. 2007, Komossa & Xu 2007). Any such study would involve one important step: the distinction between true outliers from the $M_{\text{BH}} - \sigma$ relation on the one hand, and apparent outliers on the other hand. Apparent outliers would only appear to be off-set from the $M_{\text{BH}} - \sigma$ relation because either the choice of line width as a measure of stellar velocity dispersion was unsuitable, or the choice of line and continuum parameters as a measure of black hole mass was unsuitable. KX07 have shown that those NLS1 galaxies of their sample which deviate significantly from the $M_{\text{BH}} - \sigma$ relation of normal (and BLS1) galaxies are all characterized by high [OIII] blueshifts. While these [OIII] lines were therefore not suited as surrogate for stellar velocity dispersion, the [SII]-based measurements of

velocity dispersion of the very same objects still located them on the $M_{\text{BH}} - \sigma$ relation. Almost all galaxies which deviate most strongly from the $M_{\text{BH}} - \sigma$ relation (see our Fig. 1) show $v_{[\text{OIII}]} > 150 \text{ km s}^{-1}$. These six objects, plus three additional ones which also show $v_{[\text{OIII}]} > 150 \text{ km s}^{-1}$ define the nine blue outliers that are the target of the present study.

In order to measure systematically the deviation of a galaxy from the $M_{\text{BH}} - \sigma_*$ relation, we define the quantity $\Delta\sigma := \log \sigma_{\text{obs}} - \log \sigma_{\text{pred}}$ (as in KX07), where σ_{obs} is the observed emission-line velocity dispersion, and σ_{pred} is the stellar velocity dispersion predicted from the $M_{\text{BH}} - \sigma_*$ relation of Ferrarese & Ford (2005). We find a strong correlation between [OIII] blueshift $v_{[\text{OIII}]}$ and $\Delta\sigma$ (Fig. 1). This finding demonstrates that [OIII] velocity shift systematically affects the deviation of an object from the $M_{\text{BH}} - \sigma$ relation (see also Boroson 2005). We further find that a correlation between L/L_{Edd} and $\Delta\sigma$ (e.g., Mathur & Grupe 2005, Greene & Ho 2005; see also Netzer & Trakhtenbrot 2007) is only present in our sample if we include blue outliers; when they are removed from the sample, no correlation remains (last panel of our Fig. 4, see also KX07).

Two of our NLS1 blue outliers have independent BH mass estimates. From X-ray variability, Czerny et al. (2001) estimated $\log M_{\text{BH}} = 5.9$ for PG1244+062 which agrees well with our estimate from applying the $R_{\text{BLR}} - L$ relation ($\log M_{\text{BH}} = 6.2$). For RX01354-0043 we directly measured σ_* from stellar absorption lines (see Appendix). The value agrees well with $\sigma_{[\text{SiII}]}$ and puts RXJ01354-0043 almost perfectly on the $M_{\text{BH}} - \sigma_*$ relation (Fig. 1).

These findings demonstrate the importance of measuring [OIII] blueshifts, and removing objects with high blueshifts from a sample before putting it on the $M_{\text{BH}} - \sigma_{[\text{OIII}]}$ relation. The independent question arises as to what may cause the blueshifts of these [OIII] outliers.

4.2. Blue outliers: trends and correlations

The phenomenon of slightly different blueshifts and line widths of NLR emission lines has been recognized since the early days of AGN spectroscopy and is generally traced back to a certain stratification of the NLR in the sense that high-ionization lines are produced preferentially at small distances from the core, while low-ionization lines are preferentially produced at larger radii (e.g., Osterbrock 1991). The presence of a strong [OIII] blueshift on the order of several hundred km s^{-1} was noticed early in the prototype NLS1 galaxy IZw1³ (e.g., Phillips 1976, Véron-Cetty et al. 2004). The galaxy also shows very blueshifted IR coronal lines (Schinnerer et al. 1998) and blueshifted UV high-ionization broad lines (Laor et al. 1997).

Several recent studies systematically examined the phenomenon of blue outliers in larger samples of type 1 Seyfert galaxies (Zamanov et al. 2002, Marziani et al. 2003, Aoki et al. 2005, Boroson 2005, Bian et al. 2005). According to these studies blue outliers have high Ed-

dington ratios and small BLR Balmer line widths. However, not all sources with high Eddington ratios are blue outliers. While Bian et al. (2005) further reported a correlation between blueshift and Eddington ratio of their 7 blue outliers, Aoki et al. (2005) did not find such a correlation for 16 objects. A strong correlation between [OIII] blueshift and [OIII] line width is often seen, and is usually interpreted as evidence for outflows. Zamanov et al. (2002) noticed that most of their blue outliers also show high blueshifts in CIV1549 (but this phenomenon is not exclusive to blue outliers; Sulentic et al. 2007). Aoki et al. (2005) reported a trend that blue outliers have high black hole masses ($> 10^7 M_{\odot}$). All previous studies of samples of blue outliers focused on the [OIII]-H β spectral region in order to explore the phenomenon, with the exception of Boroson (2005). Although Boroson (2005) measured the positions of other NLR lines in order to establish a systemic reference for the [OIII] line properties, we have, for the first time, measured the widths and strengths of all the optical NLR lines in blue outliers in order to study the nature of blue outliers and explore the dynamics of the NLR.

For each galaxy, we find a strong correlation between emission line blueshift and ionization potential of the line-emitting ion. Coincidentally, higher ionization potentials of the ions in question also come with higher critical densities of the forbidden line transitions observed from the respective ions. Therefore, a correlation between outflow velocity and ionization potential would generally imply a correlation with critical density, and vice versa, raising the question which of the two is the fundamental correlation; density stratification or ionization stratification. An important exception to the above rule is [OI]6300, which has zero ionization potential, while its critical density ($n_{\text{crit}} = 1.8 \cdot 10^6 \text{ cm}^{-3}$) is relatively high. [OI] is detected in several of our NLS1 galaxies, and we find that [OI] follows the trend in ionization potential, but not in critical density, arguing that the former correlation is the underlying one (Fig. 3)⁴. We confirm the previously known correlation between [OIII] blueshift and line width.

Blue outliers only occur among the NLS1 galaxies of our sample (i.e., sources with high Eddington ratios and small Balmer line widths), but within the NLS1 population, blue outliers do not show a strong correlation with Eddington ratio even though they preferentially avoid low ratios. No correlation of outflow velocity with black hole mass, absolute magnitude, and with the width of the broad component of H β is found. Like in other samples, the number of objects is small, and larger samples of blue outliers are needed to confirm the weak trends.

It has occasionally been suggested that [OIII] in blue outliers appears broadened by orientation effects in the sense that we look face-on on the central engine, and into an outflow (Zamanov et al. 2002, Marziani et al. 2003, Boroson 2005). If that scenario is correct, we can use blue outliers as test-beds for orientation-dependent models of NLS1 galaxies which allow for the possibility that the H β line of NLS1 galaxies is narrowed due to viewing angle effects. If, in blue outliers, the BLR was in a plane

³ It is also known in some radio galaxies [e.g., PKS1549-79 (Tadhunter et al. 2001, Holt et al. 2006), IC5063 (Morganti et al. 2007), and PKS0736+01 (Zamanov et al. 2002, Marziani et al. 2003)]. Also note systematic blueshifts in high-ionization BLR emission lines in quasar samples (e.g., Gaskell 1982, Sulentic et al. 2007).

⁴ It is well possible that we have both, ionization and density stratification. In that case, the inner high-density clouds are also highly ionized and/or matter-bounded, with little [OI] left.

and if we viewed it face-on, blue outliers should have the smallest $H\beta$ widths among NLS1 galaxies (here, we temporarily classify NLS1 galaxies independently of their $H\beta$ width, but only use the ratios $[OIII]/H\beta$ and $FeII/H\beta$ which still makes all of our blue outliers NLS1 galaxies: in all cases $[OIII]/H\beta_{totl} < 3$, and $FeII/H\beta_{totl} > 0.5$). However, we do not find any trend for small widths of the broad Balmer lines among the objects of our sample (see Fig. 4).

The $[OIII]$ lines of several objects still show the phenomenon of blue wings, arguing against the previous suggestion that the classical $[OIII]$ emission in blue outliers is absent and we actually only see the blue wing. [However, occasionally, the presence of a strong blue wing could mimic a blue outlier, if the wing is not spectroscopically resolved from the core of the line (e.g., Grandi 1977, Holt et al. 2003)].

4.3. Models of the narrow-line region

There is good evidence that the motion of NLR clouds is strongly influenced by the bulge gravitational potential (e.g., Véron 1981, Whittle et al. 1992, Nelson & Whittle 1996; see the prev. Sect. 4.1). At the same time, there is also evidence for radial motions in NLRs based for instance on blue asymmetries of $[OIII]$ profiles (e.g., de Robertis & Osterbrock 1984, Veilleux 1991, Whittle 1992, Véron-Cetty et al. 2001), on correlations of blue wing blueshift with the Eddington ratio and other arguments (Xu et al. 2007), and on spatially resolved $[OIII]$ velocity shifts (e.g., Schulz 1990, Das et al. 2005). The existence of $[OIII]$ blue wings can formally be equally well interpreted in terms of inflows or outflows, plus selective obscuration. Generally, there is a preference for the outflow interpretation.

Regarding theoretical models for outflows, a lot of work has focussed on magnetocentrifugal winds and radiatively driven outflows from the accretion disk region (see Königl 2006, Everett 2007, Proga 2007 for reviews). These models have successfully been applied to BAL flows and the BLR emission lines, are supported by recent observations (Young et al. 2007), and have recently been extended to spatial scales typical of the very inner NLR (Proga et al. 2008). However, little is known about the formation or continuation of such winds on much larger scales on the order of 100 pc – kpc characteristic for NLRs. Mechanisms suggested to be relevant in the NLR (and CLR) include radiation pressure acting on gas (Binette et al. 1997, Das et al. 2007) and on dust grains embedded in the clouds (Binette 1998, Dopita et al. 2002), and the entrainment of NLR clouds in hot winds (Krolik & Vrtilik 1984, Schiano 1986, Mathews & Veilleux 1989, Smith 1993, Everett & Murray 2007). The presence of collimated outflows of radio plasma in form of jets and their local interaction with NLR clouds has been observed directly (e.g., Falcke et al. 1998). Spatially resolved imaging spectroscopy of nearby AGN has produced several good examples of spatial coincidences between radio jets and line blueshifts (e.g., Riffel et al. 2006, Morganti et al. 2007), while in other cases the jet-cloud interaction is very weak and does not significantly affect the local NLR velocity field (e.g., Cecil et al. 2002, Das et al. 2005). In some cases, jets are absent but emission lines are still blueshifted (Barbosa et al. 2008, in prep). In AGN with strong starburst activity winds

could also be starburst driven (e.g., Rupke et al. 2005).

Regarding NLS1 galaxies, their high Eddington ratios make the presence of radiation-pressure driven *winds* (on the accretion disk scale) very likely. Less certain and understood is the efficiency of *jet* launching under high-accretion rate conditions. Again, these mechanisms refer to the innermost AGN region, not to larger scales. Blue outliers with their extreme velocity shifts place particularly tight constraints on models for AGN outflows on large, i.e. NLR, scales. We discuss several NLR models for blue outliers in turn.

4.3.1. A compact NLR ?

Zamanov et al. (2002) and Marziani et al. (2003) suggested that blue outliers possess a very compact NLR, perhaps the result of the youth of these NLS1 galaxies which did not yet develop a full NLR. Their idea was based on the assumption that blue outliers would only possess $[OIII]$ emission and lack other narrow emission lines. However, we do find a classical NLR in terms of the presence of low-ionization lines. Further, the fact that their $[SII]$ line widths put the blue outliers on the same $M_{BH} - \sigma$ relation with BLS1 and normal galaxies strongly indicates that their outer NLR is a quiescent classical NLR similar to that of other BLS1 and NLS1 galaxies.

4.3.2. A two-component NLR

The strong blueshifts we detect in the high-ionization component raises the possibility that we see two independent components; a classical NLR, plus an independent outflow component which could be due to a disk wind, a wind from the torus or in form of a lowly ionized warm absorber. However, this interpretation is very unlikely, because the non-blueshifted $[OIII]$ counterpart to the low-ionization lines, as it would be expected from *the inner part* of a classical NLR, is weak or absent. This fact leads us almost inevitably to the third and fourth possibility.

4.3.3. A classical NLR, modified at small radii

The fact that we do not detect a classical inner NLR, in form of a second, non-blueshifted $[OIII]$ emission component, implies that processes directly modify/disturb at least the inner NLR; perhaps in form of radio-jet – cloud interaction. However, the strong dependence of emission line velocity shift on ionization potential that we detect (Fig. 3) indicates that we see a highly stratified, photoionized medium, not a local interaction due to shocks and locally disturbed velocity fields.

4.3.4. NLR clouds entrained in a wind

The phenomenologically most straight-forward solution is one in which the (CLR and) NLR clouds themselves follow a decelerated outflow. This scenario requires an efficient driving mechanism and perhaps an efficient deceleration mechanism. One possibility is direct acceleration of the NLR clouds by radiation pressure acting on gas or dust; another is the presence of a hot wind which entrains the NLR clouds (see Sect. 4.4). If the wind forms a decelerating outflow, the entrained clouds of the CLR/ inner NLR would have the highest outflow velocities, respectively, which would decrease in dependence of

core distance and would leave the outer, low-ionization part of the NLR unaffected.

Zamanov et al. (2002) reported a linkage of [OIII] blue-outlierness with broad-line CIV blueshift. Could the same wind persist from the disk, to the high-ionization BLR [but leave the bulk of the BLR unaffected; by blowing perpendicular?], and on to the CLR and inner NLR?

In this picture, the NLRs of BLS1 galaxies, NLS1s, and blue outliers would be intrinsically similar, and the motion of NLR clouds generally dominated by the bulge gravitational potential. Which emission line regions partake in an outflow would depend on the efficiency/operating distance of the wind. It could be present in all AGN, but would generally only affect the CLR (in AGN with blueshifted iron coronal lines but quiescent NLRs), or level off even before reaching the CLR.

4.4. Mechanisms of cloud acceleration and entrainment

While phenomenologically successful, the question is raised as to the origin of the wind/outflow on the one hand, and the entrainment mechanism and cloud stability against disruptive instabilities (Mathews & Veilleux 1989, Schiano et al. 1995) on the other hand. We discuss several possibilities in turn.

Cloud acceleration by radiation pressure acting on dust— Radiation pressure acting on dust grains embedded in the gas clouds is an efficient way of cloud acceleration (e.g., Binette 1998, Dopita et al. 2002, Fabian et al. 2006). In blue outliers, this mechanism is likely not at work, because we do not expect dust in the high-ionization BLR (we are assuming here that the high-ionization part of the BLR partakes in the outflow, motivated by the results of Zamanov et al. (2002) described in Sect. 4.3.4). Some dust might be present in the CLR (even a small admixture of dust would still lead to efficient radiative acceleration, and generally still predict sufficiently strong gas-phase iron lines; Binette 1998). While, observationally, dust-rich NLRs could be present in individual blue outliers (e.g., RXJ0135–0043), most of them have very blue optical continua arguing against the presence of an excess of dusty gas along the line of sight. These arguments make cloud acceleration by radiation pressure acting on dust grains an unlikely scenario.

Cloud entrainment in collimated radio plasma— Outflowing radio plasma in form of jets is known to be present and to reach large distances from the nucleus in AGN, so could plausibly affect several emission-line regions on its way. The phenomenon of cloud entrainment in radio plasma has been directly observed and studied in star-forming regions (Ostriker et al. 2001, Stojimirović et al. 2006). Jet-cloud interaction can result in a variety of phenomena, including cloud entrainment, jet deflection and disruption and cloud destruction (e.g., Saxton et al. 2005, Krause 2007 and references therein). Of interest here is entrainment (Blandford & Königl 1979, Schiano et al. 1995, Fedorenko et al. 1996). One key problem is cloud longevity against various instabilities. Fedorenko et al. (1996) argued for magnetic NLR confinement which would then allow for NLR cloud entrainment in radio jets.

Independent of theoretical considerations the question

is raised if the blue outliers of our sample all harbor powerful radio jets. Relatively little is known about the radio properties of NLS1 galaxies in general. On average, they tend to be less radio-loud than BLS1 galaxies (Zhou et al. 2006, Komossa et al. 2006) and share some similarities with compact steep spectrum radio sources (Komossa et al. 2006). Four of the blue outliers of our sample have FIRST radio detections. These imply radio powers of $P_{1.4} = 10^{22} - 8 \cdot 10^{23} \text{ W Hz}^{-1}$ (Tab. 1) at 1.4 GHz; similar to those AGN which Nelson & Whittle (1996) find to be off-set from the $M_{\text{BH}} - \sigma_*$ relation. We do not have information on the radio morphology of the blue outliers. Sources are unresolved with FIRST, with one remarkable exception: the radio emission of RXJ0135–0043 is extended by ~ 10 kpc (or double; see Appendix). Spatially resolved radio observations of the sources are required to search for the presence of jets and to study the radio properties in more detail.

Thermal winds— Variants of thermal wind models have been studied in order to explain the kinematics of ionized absorbers (Chelouche & Netzer 2005), and of NLRs. *Isothermal* Parker wind models of Everett & Murray (2007), originally computed in order to model spatially resolved NLR velocity gradients of NGC 4151 (Das et al. 2005), would have roughly the right properties to explain our average blue outlier velocity shifts and radial velocity changes. A range in NLR cloud column densities would lead to a spread in cloud velocities (see Eqn. (10) of Everett & Murray 2007), thereby perhaps explaining the observed line broadening. However, as also shown by Everett & Murray (2007), realistic models including photoionization heating have temperature gradients, and adiabatic cooling decelerates the winds too quickly. An extra heating source of unknown nature would be needed in order to keep the wind isothermal. Models of Das et al. (2007), based on radiative acceleration of NLR clouds, implied that NLR clouds do not decelerate quickly enough in order to explain NLR velocity gradients of NGC 1068 observed with HST; models work after introducing drag forces from an ambient medium. Detailed modeling of the present data would likely involve several of the above model ingredients. Such modelling is beyond the scope of this paper.

High Eddington ratios and orientation effects— Common to blue outliers is their high Eddington ratios. Could high L/L_{Edd} be the wind driving mechanism? Additional orientation effects (as also discussed by Marziani et al. 2003, Boroson 2005) are still needed in order to explain why not all AGN with high L/L_{Edd} are blue outliers. Near face-on orientation would have us look more down the flow in blue outliers, thereby enhancing the stratification, broadening, and blueshift effect.

4.5. Links with (compact) radio sources and mergers

It is interesting to point out similarities between the phenomenon of blue outliers in NLS1 galaxies and in radio galaxies (see also Holt et al. 2006). Several radio galaxies show a similar phenomenon of high [OIII] core blueshifts and line broadening (e.g., Tadhunter et al. 2001, Marziani et al. 2003, Holt et al. 2006, Stockton et al. 2007; see Gupta et al. 2005 for a related phenomenon in the UV). Jet-cloud interaction in the (inner) NLR is the favored interpretation of most of these

sources. These objects may represent the early stages of radio-source evolution (Tadhunter et al. 2001). Radio galaxies with blue outliers in [OIII] are typically compact flat spectrum sources, are absorbed, and are luminous in the infrared. For some (e.g., PKS1549–79 and PKS0736+01) there is evidence that we have a near face-on view (Tadhunter et al. 2001, Marziani et al. 2003). As pointed out before, the strong stratification we see in NLS1 blue outliers argues against local jet-cloud interactions in those galaxies, but would be consistent with NLR clouds entrained in the outflowing radio plasma.

The blue outliers among the radio galaxies show signs of recent mergers. Regarding NLS1 galaxies in general, there is no evidence that the majority of them underwent recent mergers or has an excess of companion galaxies (Krongold et al. 2001, Ryan et al. 2007). Little is known about the host galaxies of our blue outlier sample, in particular. IRAS11598-0112 indeed is a merger with prominent tidal tails (Veilleux et al. 2002), ultraluminous in the infrared. Inspecting the SDSS images of the other galaxies of our sample we do not find strongly disturbed galaxy images indicating ongoing mergers, but this needs to be confirmed with deeper imaging. One galaxy, RXJ0135–0043, shows indications of an off-center nucleus. That effect could be caused by interaction, be mimicked by dust, or have another origin.

4.6. Recoiled Black Holes ?

Recent simulations of merging black holes predict black hole recoil velocities due to emission of gravitational wave radiation up to several thousand km s^{-1} (e.g., Campanelli et al. 2007; review by Pretorius 2007). Potentially, high relative outflow velocities of AGN emission line regions vs the host galaxy can arise if the recoiled black hole keeps its BLR and inner NLR (Bonning et al. 2007). Applied to blue outliers, if they harbored recoiled BHs, their whole BLR (plus the high-ionization NLR) should show high blueshifts, while the ‘remnant’ NLR would still appear in low-ionization lines. In that case, we expect the broad component of the Balmer lines to exhibit the highest blueshifts of all emission lines; which is, however, not observed. Shifts in broad $\text{H}\beta$ are less than those in [OIII].

4.7. Future work

The SDSS data base is well suited for a systematic search for more blue outliers. Zhou et al. (2006) mention in passing the presence of several extreme ones among their NLS1 galaxy sample but do not discuss them further. Spatially resolved optical spectroscopy will allow us to measure directly line widths, outflow velocities, etc. in dependence of the core distance⁵. Spectroscopy in the IR and UV will tell whether trends (a correlation with ionization potential) persist in IR coronal lines and high-ionization UV broad lines. X-ray measurements of blue outliers will be useful to search for signs of high-velocity ionized outflows, and to see whether blue outliers again stick out in AGN correlation space when adding their X-ray properties (X-ray steepness, variability) to correlation analyses. (High-resolution) radio observations of all galaxies will facilitate further comparison between blue

outliers in radio galaxies and NLS1 galaxies and will tell whether radio jets are present in NLS1 blue outliers. Radio observations have the potential to confirm the pole-on hypothesis of blue outliers, if relativistic beaming is detected. Imaging with HST will reveal whether the host galaxies of blue outliers show signs of recent mergers. In particular, galaxy merger simulations predict strong outflows in the final merger phase (e.g., Springel et al. 2005). Imaging will allow us to test whether blue outliers are in such a phase.

If the face-on interpretation of blue outliers is correct, they are also useful test-beds for the question, whether the width of broad $\text{H}\beta$ is systematically affected by orientation. Increasing the sample size will allow us to test more stringently whether the broad component of $\text{H}\beta$ is systematically narrower in blue outliers. If so, this would imply that BLR clouds are arranged in a plane, and we would underestimate systematically the BH masses in these objects, and perhaps NLS1 galaxies in general. If, instead, their BLR is spherical, we would not see systematically narrower $\text{H}\beta$ in objects viewed face-on, and would not have to worry about correctness of BH mass estimates. Our preliminary results indicate that the latter is the case.

On the theoretical side, the question is raised as to which winds can operate across long distances spanning the high-ionization BLR, CLR and a substantial part of the NLR, predict the observed gradient in cloud velocities ($\sim 1000 \text{ km s}^{-1}$ of high-ionization emission-line clouds close to the nucleus, and several hundred km s^{-1} further out on typical NLR scales while the outer NLR is mostly unaffected), and ensure longevity of the emission-line clouds.

5. SUMMARY AND CONCLUSIONS

In [OIII] blue outliers with their extreme velocity shifts the effects of secondary influences on the NLR kinematics are enhanced or dominate completely. Their study is therefore of great relevance for (1) scrutinizing the usefulness and limitations of [OIII] width as a proxy for stellar velocity dispersion; (2) understanding the origin and dynamics of the NLR; (3) investigating driving mechanisms of AGN outflows on large scales; and (4) examining possible links with results from merger simulations which predict that a substantial fraction of the ISM of the merger should be outflowing. We have systematically studied the optical properties of such AGN with high [OIII] blueshifts which deviate from the $M_{\text{BH}} - \sigma_{[\text{OIII}]}$ relation of BLS1 and NLS1 galaxies, and obtained the following results:

- All of them have high Eddington ratios ($L/L_{\text{edd}}=0.5-1.5$) and narrow BLR Balmer lines ($\text{FWHM}(\text{H}\beta_{\text{b}})=1200-1800 \text{ km s}^{-1}$), which makes them NLS1 galaxies. The fraction of blue outliers among our NLS1 sample is 16% ($v_{[\text{OIII}]} \gtrsim 150 \text{ km s}^{-1}$), and 5% at the highest outflow velocities ($v_{[\text{OIII}]} \gtrsim 250 \text{ km s}^{-1}$). While blue outliers do enhance correlations which appear across the whole BLS1-NLS1 population, we do not find strong correlations of [OIII] outflow velocity with the Eddington ratio within the blue outlier population itself; perhaps due to the small sample size.

- We do detect a strong correlation between emission-line blueshift and ionization potential, and confirm a

⁵ This approach is difficult, however, if the near-pole-on interpretation of blue outliers is correct.

strong correlation between [OIII] blueshift and [OIII] line width. The presence of a classical quiescent *outer* NLR is indicated by the existence of low ionization lines, by [SII] line widths which locate the blue outliers on the same $M_{\text{BH}} - \sigma_{[\text{SII}]}$ relation as other BLS1 and NLS1 galaxies, and by inferred NLR densities similar to other NLS1 galaxies. On the other hand, zero-blueshift [OIII] emission expected from a quiescent *inner* NLR is weak or absent.

- Taken together, these observations place tight constraints on models: We favor a scenario where NLR clouds of blue outliers are entrained in a decelerating wind. Similar, less powerful winds could be present in all AGN, but would generally only affect the CLR (in AGN with blueshifted iron coronal lines but quiescent NLRs), or level off even before reaching the CLR only affecting the high-ionization BLR.

- The mechanism that drives and decelerates the wind is speculative at present, but could be linked to the high Eddington ratios of the galaxies. Extra orientation effects (near pole-on views), considered previously to explain the correlation of [OIII] blueshift with line width of blue outliers, would also explain the strong ionization stratification we detect.

- Two blue outliers have independent BH mass / stellar velocity dispersion measurements and these place them on or close to the $M_{\text{BH}} - \sigma$ relation of non-active galaxies. This, together with the fact that the width of broad H β does not correlate with [OIII] outflow velocity, indicates: If blue outliers are indeed seen more face-on, this fact does not reflect strongly in their H β widths, implying that their BLR geometry is closer to spherical than to planar.

- Most remarkable among the blue outliers is the galaxy RXJ01354–0043. Unlike other NLS1 galaxies its radio emission is extended and possibly double, its optical Balmer lines appear to be double-peaked, and its optical spectrum shows strong absorption lines from the host galaxy. The link between blue outliers in NLS1 galaxies and in (compact) radio galaxies needs further exploration.

6. APPENDIX: NOTES ON INDIVIDUAL OBJECTS

A few sources are included in the SDSS-NLS1 samples of Williams et al. (2002) and Anderson et al. (2003). The high [OIII] blueshifts of SDSSJ115533.50+010730.4 and RXJ01354–0043 were reported by Bian et al. (2005). Boroson (2005) measured [OIII] blueshifts of NGC450#86, RXJ01354–0043, PG1244+026, and SDSS17184+5734. Here, we provide a short summary of the multi-wavelength properties of the blue outliers collected from the literature, and give some comments based on our optical spectral analysis. Galaxies are listed in order of decreasing [OIII] blueshift.

SBS0919+515 — This AGN is a known X-ray source, first detected with the Einstein observatory (Chanan et al. 1981), mostly studied in the X-ray regime (e.g., Boller et al. 1996, Vaughan et al. 2001), and optically identified as NLS1 galaxy by Stephens (1989). It shows the highest [OIII] blueshift of our sample ($v_{[\text{OIII}]} = 430 \text{ km s}^{-1}$).

SDSSJ115533.50+010730.4 — This AGN was detected in X-rays during the ROSAT all-sky survey (Voges et al.

1999) and was first classified as NLS1 galaxy by Williams et al. (2002). It has the second-highest [OIII] velocity shift of our sample ($v_{[\text{OIII}]} = 330 \text{ km s}^{-1}$), highly blueshifted [NeV], and faint coronal line emission of [FeX] with a blueshift corresponding to $v_{[\text{FeX}]} \approx 1000 \text{ km s}^{-1}$, among the highest blueshifts reported for coronal lines to date.

RXJ01354–0043 (SDSSJ013521.68–004402.2) — This AGN was detected in the X-ray and radio band (Brinkmann et al. 2000, Wadadekar 2004) and was optically identified as NLS1 galaxy by Williams et al. (2002). It is remarkable in several respects. We find that its optical spectrum appears to be dominated by the host galaxy. Strong absorption lines from higher order Balmer lines, Ca H&K and NaID are detected (Fig. 5). The optical AGN continuum emission is either intrinsically weak, or absorbed (which would require a peculiar geometry of the absorber, given that the broad Balmer lines are present). RXJ01354–0043 is detected with GALEX⁶ and displays red UV colors. Its (narrow) Balmer lines appear double-peaked, with a separation of $\sim 580 \text{ km s}^{-1}$, or else are affected by residual, exceptionally strong and redshifted, host-galaxy features which is very unlikely, given the strength of H α . The line decomposition shown in Fig. 5 assumes the same widths of the narrow core of H β and of the two [NII] lines, fixed to the width of [SII], and further assumes a fixed [NII] line ratio. The remaining profile was modeled with two Gaussians of free parameters and can be well fit with a broad component plus a second, redshifted relatively narrow component. RXJ01354–0043 has a FIRST detection with a radio flux of 2 mJy and there is evidence for extended radio emission (Becker et al. 1997⁷), corresponding to a scale of $\sim 10 \text{ kpc}$. This is remarkable because few if any NLS1 galaxies are known to have widely extended radio emission (Ulvestad et al. 1995, Komossa et al. 2006, Yuan et al. 2008). Inspecting the FIRST image cut-out, the source appears to be double. Among the emission lines, only the Balmer lines appear double-peaked. RXJ01354–0043 is the first blue outlier to show this phenomenon. Explanations include jet-cloud interaction, a bipolar outflow or, speculatively, superposed strong Balmer absorption (which is rarely seen because the required level population is not easy to achieve; Hall 2007, Lu et al. in prep.). We have used the stellar absorption lines from the host galaxy for a measurement of σ_* . We obtain $\sigma_* = 82 \text{ km s}^{-1}$ which is in good agreement with the [SII]-based measurement, $\sigma_{[\text{SII}]} = 106 \text{ km s}^{-1}$, and locates RXJ01354–0043 (almost perfectly) on the $M_{\text{BH}} - \sigma_*$ relation of non-active galaxies (Fig. 1).

NGC450#86 — Identified as NLS1 galaxy by Williams et al. (2002) and detected in X-rays during the ROSAT all-sky survey (Voges et al. 1999).

SDSSJ032606.75+011429.9 — A basically unknown galaxy, with optical NLS1 spectrum (Williams et al. 2002). No radio or X-ray detection was reported.

⁶ <http://galex.stsci.edu/GR2/>
⁷ most recent catalogue update at <http://cdsarc.u-strasbg.fr/viz-bin/Cat?VIII/71>

IRAS 11598–0112— This galaxy is ultraluminous in the infrared (Murphy et al. 1996, Kim & Sanders 1998) with a single nucleus and prominent tidal tails (Veilleux et al. 2002). Its optical spectrum is that of a NLS1 galaxy (Moran et al. 1996). It is almost radio-loud with a 1.4 GHz radio index $R \approx 5$ (Komossa et al. 2006) and was first detected in X-rays with ROSAT (Voges et al. 1999). The FeII emission in its optical spectrum is not well described by our FeII template. In particular, the ‘red’ and ‘blue’ complexes of FeII do not match each other well, and the source redshift appears to differ from that of FeII. Strong emission of unknown nature remains blueward of [OIII]. Formally, we can describe it with an extra [OIII] component, broad (FWHM([OIII])=1800 km s⁻¹) and highly blueshifted ($v=1300$ km s⁻¹). If real, it could represent an extreme blue wing, or could imply the presence of an extra starburst/shock-driven component. The structure needs to be confirmed by independent spectroscopy.

SDSSJ171828.99+573422.3— Detected with ROSAT (Brinkmann et al. 1999), and optically identified as NLS1 by Williams et al. (2002).

PG1244+026— This AGN (Green et al. 1986) is a well-known X-ray, UV, infrared and radio source (e.g., Elvis et al. 1986, Kellerman et al. 1989, Sanders et al. 1989, Fiore et al. 1998, Ballantyne et al. 2001, Jimenez-Bailón et al. 2005) with an optical NLS1 spectrum (Miller et al. 1992, Veron-Cetty et al. 2001). It is radio quiet with a 5 GHz radio index of $R = 0.5$ (Kellerman et al. 1989). Hayashida (2000) and Czerny et al. (2001) determined its black hole mass based on X-ray variability (the power density spectrum). Czerny et al. (2001) report $\log M_{\text{BH}} = 5.9$ which is consistent with our value of $\log M_{\text{BH}} = 6.2$ from applying the relation of Kaspi et al. (2005). We detect in its optical spectrum [FeX] emission with an outflow velocity of 640 km s⁻¹.

RXJ09132+3658— Detected in X-rays with ROSAT (Voges et al. 1999, Brinkmann et al. 2000) and in the radio band during the FIRST survey (Becker et al. 1997), and identified as NLS1 galaxy by Xu et al. (1999).

DX acknowledges the support of the Chinese National Science Foundation (NSFC) under grant NSFC-10503005, and the support of MPG/MPE. HZ acknowledges support from the Alexander von Humboldt Foundation, from NSFC (grant NSF-10533050), and from program 973 (No. 2007CB815405). LB acknowledges support from CONACyT grant J-50296. We thank our referee for his/her comments and suggestions, and the members of MPE’s new Physics of Galactic Nuclei group and J. Sulentic, D. Proga and D. Merritt for discussions. This research has made use of the SDSS data base, and of the NASA/IPAC Extragalactic Database (NED) which is operated by the Jet Propulsion Laboratory, California Institute of Technology, under contract with the National Aeronautics and Space Administration. Funding for the SDSS and SDSS II has been provided by the Alfred P. Sloan Foundation, the Participating Institutions, the National Science Foundation, the U.S. Department of Energy, the National Aeronautics and Space Administration, the Japanese Monbukagakusho, the Max Planck Society, and the Higher Education Funding Council for England. The SDSS is managed by the Astrophysical Research Consortium for the Participating Institutions. The Participating Institutions are the American Museum of Natural History, Astrophysical Institute Potsdam, University of Basel, University of Cambridge, Case Western Reserve University, University of Chicago, Drexel University, Fermilab, the Institute for Advanced Study, the Japan Participation Group, Johns Hopkins University, the Joint Institute for Nuclear Astrophysics, the Kavli Institute for Particle Astrophysics and Cosmology, the Korean Scientist Group, the Chinese Academy of Sciences (LAMOST), Los Alamos National Laboratory, the Max-Planck-Institute for Astronomy (MPIA), the Max-Planck-Institute for Astrophysics (MPA), New Mexico State University, Ohio State University, University of Pittsburgh, University of Portsmouth, Princeton University, the United States Naval Observatory, and the University of Washington.

REFERENCES

- Abazajian, K., et al. 2005, AJ, 129, 1755
 Anderson, S.F., et al. 2003, AJ, 126, 2209
 Aoki, K., Kawaguchi, T., & Ohta, K. 2005, ApJ, 618, 601
 Ballantyne, D.R., Iwasawa, K., & Fabian, A.C. 2001, MNRAS, 323, 506
 Barth, A.J., Greene, J.E., & Ho, L.C. 2005, ApJ, 619, L151
 Becker, R.H., Helfand, D.J., White, R.L., Gregg, M.D., & Laurent-Muehleisen, S.A. 1997, ApJ, 475, 479
 Bennert, N., Jungwiert, B., Komossa, S., Haas, M., & Chini, R. 2006, A&A, 456, 953
 Bian, W., & Zhao, Y. 2004, MNRAS, 347, 607
 Bian, W., Yuan, Q., & Zhao, Y. 2005, MNRAS, 364, 187
 Binette, L. 1998, MNRAS, 294, L47
 Binette, L., Wilson, A.S., Raga, A., Storchi-Bergmann, T., 1997, A&A, 327, 909
 Blandford, R., & Königl, A. 1979, ApL, 20, 15
 Boller, T., Brandt, W.N., & Fink, H., 1996, A&A, 305, 53
 Bonning, E.W., Shields, G.A., & Salvander, S. 2007, ApJ, 666, L13
 Boroson, T.A. 2002, ApJ, 565, 78
 Boroson, T.A. 2003, ApJ, 585, 647
 Boroson, T.A. 2005, ApJ, 130, 381
 Botte, V., Ciroi, S., Rafanelli, P., & Di Mille, F. 2004, AJ, 127, 3168
 Botte, V., Ciroi, S., Di Mille, F., Rafanelli, P., & Romano, A., 2005, MNRAS, 356, 789
 Brinkmann, W., et al. 1999, A&AS, 134, 221
 Brinkmann, W., et al. 2000, A&A, 356, 445
 Campanelli, M., Lousto, C.O., Zlochower, Y., & Merritt, D. 2007, PhRvL, 98, 1102
 Cecil, G., et al. 2002, ApJ, 585, 627
 Chanan, G.A., Margon, B., & Downes R.A. 1981, ApJ, 243, L5
 Chelouche, D., & Netzer, H. 2005, ApJ, 625, 95
 Churazov, E., Brüggem, M., Kaiser, C.R., Böhringer, H. & Forman, W. 2001, ApJ, 554, 261
 Colbert, E.J.M., et al. 1996, ApJS, 105, 75
 Crenshaw, D.M., & Kraemer, S.B. 2007, ApJ, 659, 250
 Czerny, B., Nikolajuk, M., Piasecki, M., & Kuraszekiewicz, J. 2001, MNRAS, 325, 865
 Das, V., et al. 2005, AJ, 130, 945
 Das, V., Crenshaw, D.M., & Kraemer, S.B. 2007, ApJ, 656, 699
 de Robertis, M., & Osterbrock, D.E. 1984, ApJ, 286, 171
 di Matteo, T., Springel, V., & Hernquist, L. 2005, Nature, 433, 604

- Dopita, M., Groves, B.A., Sutherland, R.S., Binette, L., & Cecil, G. 2002, *ApJ*, 572, 753
- Elvis, M., et al. 1986, *ApJ*, 310, 291
- Elvis, M. 2000, *ApJ*, 545, 63
- Elvis, M. 2006, *MemSAIt*, 77, 573
- Erkens, U., Apenzeller, I., & Wagner, S. 1997, *A&A*, 323, 707
- Everett, J.E. 2007, *Ap&SS*, 311, 269
- Everett, J.E., & Murray, N. 2007, *ApJ*, 656, 93
- Fabian, A. 1999, *MNRAS*, 308, L39
- Fabian, A., Celotti, A., & Erlund, M.C. 2006, *MNRAS*, 373, L16
- Falcke, H., Wilson, A.S., & Simpson, C. 1998, *ApJ*, 502, 199
- Fedorenko, V.N., Paltani, S., & Zentsova, A.S. 1996, *A&A*, 314, 368
- Ferrarese, L., & Merritt, D. 2000, *ApJ*, 539, L9
- Ferrarese, L., & Ford, H. 2005, *Space Science Reviews*, 116, 523
- Fiore, F., et al. 1998, *MNRAS*, 298, 103
- Gaskell, C.M. 1982, *ApJ*, 263, 79
- Gallimore, J.F., Axon, D.J., O'Dea, C., Baum, S.A., & Pedlar, A. 2006, *AJ*, 132, 546
- Gebhardt, K., et al. 2000, *ApJ*, 539, L13
- Green, R.F., Schmidt, M., & Liebert, J. 1986, *ApJS*, 61, 305
- Greene, J.E., & Ho, L.C. 2005, *ApJ*, 627, 721
- Grandi, S.A. 1977, *ApJ*, 215, 446
- Grupe, D. 2004 *AJ*, 127, 1799
- Grupe, D., & Mathur, S. 2004 *ApJ*, 606, L41
- Gupta, N., Srianan, R., & Saiki, D.J. 2005, *MNRAS*, 361, 451
- Hall, P. 2007, *AJ*, 133, 1271
- Hayashida, K. 2000, *NewAR* 44, 419
- Heckman, T.M., Miley, G.K., van Breugel, W.J.M., & Butcher, H.R. 1981, *ApJ*, 247, 403
- Holt, J., Tadhunter, C.N., & Morganti, R. 2003, *MNRAS*, 342, 227
- Holt, J., et al. 2006, *MNRAS*, 370, 1633
- Jiménez-Bailón, E., et al. 2005, *A&A*, 435, 449
- Kaspi, S., et al. 2005, *ApJ*, 629, 61
- Kaspi, S., et al. 2000, *ApJ*, 533, 631
- Kellermann, K.I., Sramek, R., Schmidt, M., Shaffer, D.B., & Green, R. 1989, *AJ*, 98, 1195
- Kim, D.-C., & Sanders, D.B. 1998, *ApJS*, 119, 41
- Komossa, S., & Schulz, H. 1997, *A&A*, 323, 31
- Komossa, S., et al. 2006, *AJ*, 132, 531
- Komossa, S., & Xu, D. 2007, *ApJ*, 667, L33 (KX07)
- Komossa, S. 2008, in: *The nuclear region, host galaxy and environment of AGN*, E. Benitez, I. Cruz-Gonzales, Y. Krongold (eds), *RevMexAA*, in press, (arXiv:0710.3326v1)
- Königl, A. 2006, *MemSAIt*, 77, 598
- Krause, M. 2007, *NewAR*, 51, 174
- Kriss, G.A. 1994, *ASP Conf. Series* 61, 437
- Krolik, J.H., & Vrtilik, J.M. 1984, *ApJ*, 279, 521
- Krongold, Y., Dultzin-Hacyan, D., & Marziani, P. 2001, *AJ*, 121, 702
- Krongold, Y., et al. 2007, *ApJ*, 659, 1022
- Laor, A., Jannuzi, B.T., Green R.F., & Boroson, T.A. 1997, *ApJ*, 489, 656
- Marziani, P., Zamanov R.K., Sulentic, J.W., & Calvani, M. 2003, *MNRAS*, 345, 1133
- Mathews, W.G., & Veilleux, S., 1989, *ApJ*, 336, 93
- Mathur, S., Kuraszkiwicz, J., & Czerny, B. 2001, *NewA*, 6, 321
- Mathur, S., & Grupe, D. 2005a, *ApJ*, 633, 688
- Mathur, S., & Grupe, D. 2005b, *A&A*, 432, 463
- Miller, P., Rawlings, S., Saunders, & R., Eales, S. 1992, *MNRAS*, 254, 93
- Moll, R., et al. 2007, *A&A*, 463, 513
- Moran, E.C., Halpern J.P., & Helfand, D.J. 1996, *ApJS*, 106, 341
- Morganti, R., Tadhunter C.N., & Oosterloo, T.A. 2005, *A&A*, 444, L9
- Morganti R., Holt, J., Daripalli, L., Oosterloo, T.A., & Tadhunter, C.N. 2007, *A&A*, in press, [arXiv:0710.1189v1]
- Murphy, T.W., et al. 1996, *AJ*, 111, 1025
- Nelson, C.H. 2000, *ApJ*, 544, L91
- Nelson, C.H., & Whittle, M. 1996, *ApJ*, 465, 96
- Netzer, H., & Trakhtenbrot, B. 2007, *ApJ*, 654, 754
- Osterbrock, D.E. 1991, *Rep.Prog.Phys.* 54, 579
- Osterbrock, D.E., & Pogge, R. 1985, *ApJ*, 297, 166
- Ostriker, E.C., Lee, C.-F., Stone, J.M., & Mundy, L.G. 2001, *ApJ*, 557, 443
- Penston, M.S., Fosbury, R.A.E., Boksenberg, A., Ward, M.J., Wilson, A.S. 1984, *MNRAS*, 208, 247
- Phillips, M.M. 1976, *ApJ*, 208, 37
- Pretorius, F. 2007, arXiv:07101338
- Proga, D. 2007, *ASP Conf. Ser.*, 373, 267
- Proga, D., Ostriker, J.P., & Kurosawa, R. 2008, *ApJ*, in press; arXiv:0708.4037v2
- Rice, M., et al. 2006, *ApJ*, 636, 654
- Riffel R.A., Storchi-Bergmann, T., Winge, C., & Barbosa, F.K.B. 2006, *MNRAS*, 373, 2
- Rodriguez-Ardila, A., Prieto, M.A., Viegas, S., & Gruenwald, R. 2006, *ApJ*, 653, 1098
- Rodriguez Hidalgo, P., Hamann, F., Nestor, D., & Shields, J. 2007, *ASP Conf. Ser.* 373, 287
- Rupke, D.S., Veilleux, S., & Sanders, D.B. 2005, *ApJ*, 632, 751
- Ryan, C.J., de Robertis, M.M., Virani, S., Laor, A., & Dawson, P.C. 2007, *ApJ*, 654, 799
- Salviander, S., Shields, G.A., Gebhardt, K., & Bonning, E.W. 2007, *ApJ*, 662, 131
- Sanders, D.B., Phinney, E.S., Neugebauer, G., Soifer, B.T., & Mathews, K. 1989, *ApJ*, 347, 29
- Saxton, C.J., Bicknell, G.V., Sutherland, R.S., & Midgley, S. 2005, *MNRAS*, 359, 781
- Scannapieco, E., Silk, J., & Bouwens, R. 2005, *ApJ*, 635, L13
- Schiano, A.V.R. 1986, *ApJ*, 302, 81
- Schiano, A.V.R., Christiansen, W.A., & Knerr, J.M. 1995, *ApJ*, 439, 237
- Schinnerer, E., Eckart, & A., & Tacconi, L.J. 1998, *ApJ*, 500, 147
- Schulz, H. 1990, *AJ*, 99, 142
- Shields, G.A., et al. 2003, *ApJ*, 535, 124
- Silk, J., & Rees, M. 1998, *A&A*, 331, L1
- Smith, S.J. 1993, *ApJ*, 411, 570
- Springel, V., Di Matteo, T., & Hernquist, L. 2005, *ApJ*, 620, L79
- Stephens, S. 1989, *AJ*, 97, 10
- Stockton, A., Canalizo, G., Fu, H., & Keel, W. 2007, *ApJ*, 659, 195
- Stojimirović, I., Narayan, G., Snell, R.L., & Bally, J. 2006, *ApJ*, 649, 280
- Sulentic, J., Bachev, R., Marziani, P., Negrete, C.A., & Dultzin, D. 2007, *ApJ*, 666, 757
- Tadhunter, C., Wills, K., Morganti, R., Oosterloo, T., & Dickson, R. 2001, *MNRAS*, 327, 227
- Terlevich, E., Diaz, A.I., & Terlevich, R. 1990, *MNRAS*, 242, 721
- Tremaine, S., et al. 2002, *ApJ*, 574, 740
- Ulvestad, J.S., Antonucci, R.R.J., & Goodrich, R.W. 1995, *AJ*, 109, 81
- Vaughan, S., Edelson, R., Warwick, R.S., Malkan, M.A., & Goad, M.R. 2001, *MNRAS*, 327, 673
- Veilleux, S. 1991, *ApJ*, 369, 331
- Veilleux, S., Kim, D.-C., & Sanders, D.B. 2002, *ApJS*, 143, 315
- Veilleux, S., Cecil G., & Bland-Hawthorn, J. 2005, *ARA&A*, 43, 769
- Véron, M.P. 1981, *A&A*, 100, 12
- Véron-Cetty, M.P., Véron, P., & Goncalves, A.C. 2001, *A&A*, 372, 730
- Véron-Cetty, M.P., & Véron, P. 2003, *A&A*, 412, 399
- Véron-Cetty, M.P., Joly, M., & Véron, P. 2004, *A&A*, 417, 515
- Voges, W., et al. 1999, *A&A*, 349, 389
- Wadadekar, Y. 2004, *A&A*, 416, 35
- Wandel, A. 2002, *ApJ*, 565, 762
- Wang T., & Lu Y. 2001, *A&A*, 377, 52
- Watson L., Mathur S., & Grupe D. 2007, *AJ*, 133, 2435
- Whittle, M. 1992, *ApJ*, 387, 109
- Williams, R.J., Pogge, R.W., & Mathur, S. 2002, *AJ*, 124, 3042
- Wyithe, J.S.B., & Loeb, A. 2003, *ApJ*, 595, 614
- Xu, D., Wei, J.Y., & Hu, J.Y. 1999, *ApJ*, 517, 622
- Xu, D., Komossa, S., Zhou, H., Wang, T., & Wei, J. 2007, *ApJ*, 670, 60
- Xu, D., et al. 2008, *AJ*, to be submitted
- Young, S., Axon, D.J., Robinson, A., Hough, J.H., & Smith, J.E. 2007, *Nat*, 450, 74
- Yuan, W., et al. 2008, *ApJ*, submitted
- Zamanov, R., et al. 2002, *ApJ*, 576, L9
- Zhou, H.-Y., et al. 2006, *ApJS*, 166, 128

TABLE 1
PROPERTIES OF [OIII] BLUE OUTLIERS

coordinates (J2000) (1) ^a	common name (2)	z (3)	Δv (4)	$w(\text{OIII}_c)$ (5)	$w(\text{H}\beta_b)$ (6)	R5007 (7)	R4570 (8)	M_{BH} (9)	L/L_{Edd} (10)	n_e (11)	$P_{1.4}$ (12)
092247.03 +512038.0	SBS0919+515	0.161	430	720	1250	0.3	1.3	6.7	1.5	10	
115533.50 +010730.6	SDSSJ11555+0107	0.198	330	780	1510	0.3	0.7	6.7	0.9	200	
013521.68 -004402.2	RXJ01354-0043	0.099	240	620	1710	1.1	0.5	6.5	0.5	90	22.7
011929.06 -000839.7	NGC 450#86	0.091	220	380	1220	0.5	0.9	6.2	0.9	200	
032606.75 +011429.9	SDSSJ03261+0114	0.128	180	530	1230	0.5	0.9	6.3	1.0	340	
120226.76 -012915.3	IRAS11598-0112	0.151	170	340	1460	0.5	2.7	6.8	1.1	110	22.9
171829.01 +573422.4	SDSSJ17184+5734	0.101	150	470	1760	0.4	0.7	6.6	0.5	30	
124635.25 +022208.8	PG1244+026	0.049	150	300	1200	0.6	0.8	6.2	0.9	400	22.1
091313.73 +365817.3	RXJ09132+3658	0.108	150	350	1680	1.0	0.5	6.5	0.5	40	22.5

^a columns from left to right: (1) SDSS optical coordinates in RA (h,m,s) and DEC (d,m,s), (2) galaxy name, (3) redshift determined from H β , (4) [OIII]_{core} velocity (blueshift) wrt. [SII] in km s⁻¹, (5) FWHM([OIII]_c) in km s⁻¹, (6) FWHM(H β _b) in km s⁻¹, (7) ratio of total [OIII] over total H β emission, (8) ratio of FeII4570 over total H β emission, (9) logarithm of black hole mass in solar masses, (10) Eddington ratio, (11) NLR electron density in cm⁻³, (12) logarithm of the radio power at 1.4 GHz in W/Hz of galaxies detected in the FIRST survey.

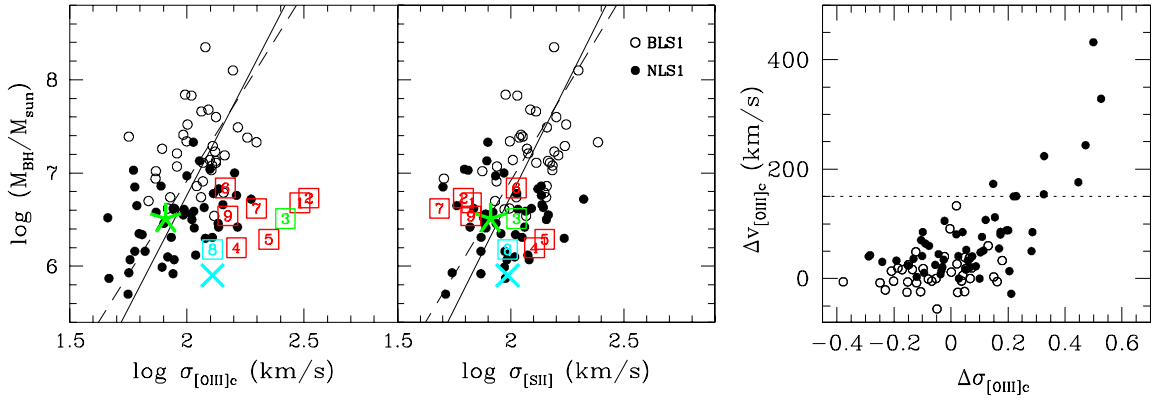


FIG. 1.— Location of blue outliers (open squares) on the $M_{\text{BH}} - \sigma$ plane in comparison to the full NLS1 (filled circles) and BLS1 (open circles) sample (Komossa & Xu 2007). *Left*: The leftmost panel is based on σ measurements from the narrow core of [OIII] λ 5007 (asymmetric blue wings were removed). Blue outliers in [OIII] (with radial velocities larger than 150 km s⁻¹) are marked with an open square. Object names are coded by number (1=SBS0919+515, 2=SDSSJ11555+0107, 3=RXJ01354-0043, 4=NGC 450#86, 5=SDSSJ03261+0114, 6=IRAS11598-0112, 7=SDSSJ17184+5734, 8=PG1244+026, 9=RXJ09132+3658). The second panel shows the same relation based on [SII]. NLS1 and BLS1 galaxies follow the same $M_{\text{BH}} - \sigma_{[\text{SII}]}$ relation. The dashed and solid lines represent the $M_{\text{BH}} - \sigma_*$ relation of non-active galaxies of Tremaine et al. (2002) and of Ferrarese & Ford (2005; FF05), respectively. Two objects with independent BH mass (PG1244+026) and stellar velocity dispersion (RXJ01354-0043) estimates are marked with special symbols (blue cross: PG1244+026, green asterisk: RXJ01354-0043). *Right*: Deviation $\Delta\sigma$ of NLS1 and BLS1 galaxies from the $M_{\text{BH}} - \sigma_*$ relation of FF05 in dependence of [OIII] radial velocity, Δv , measured w.r.t. [SII].

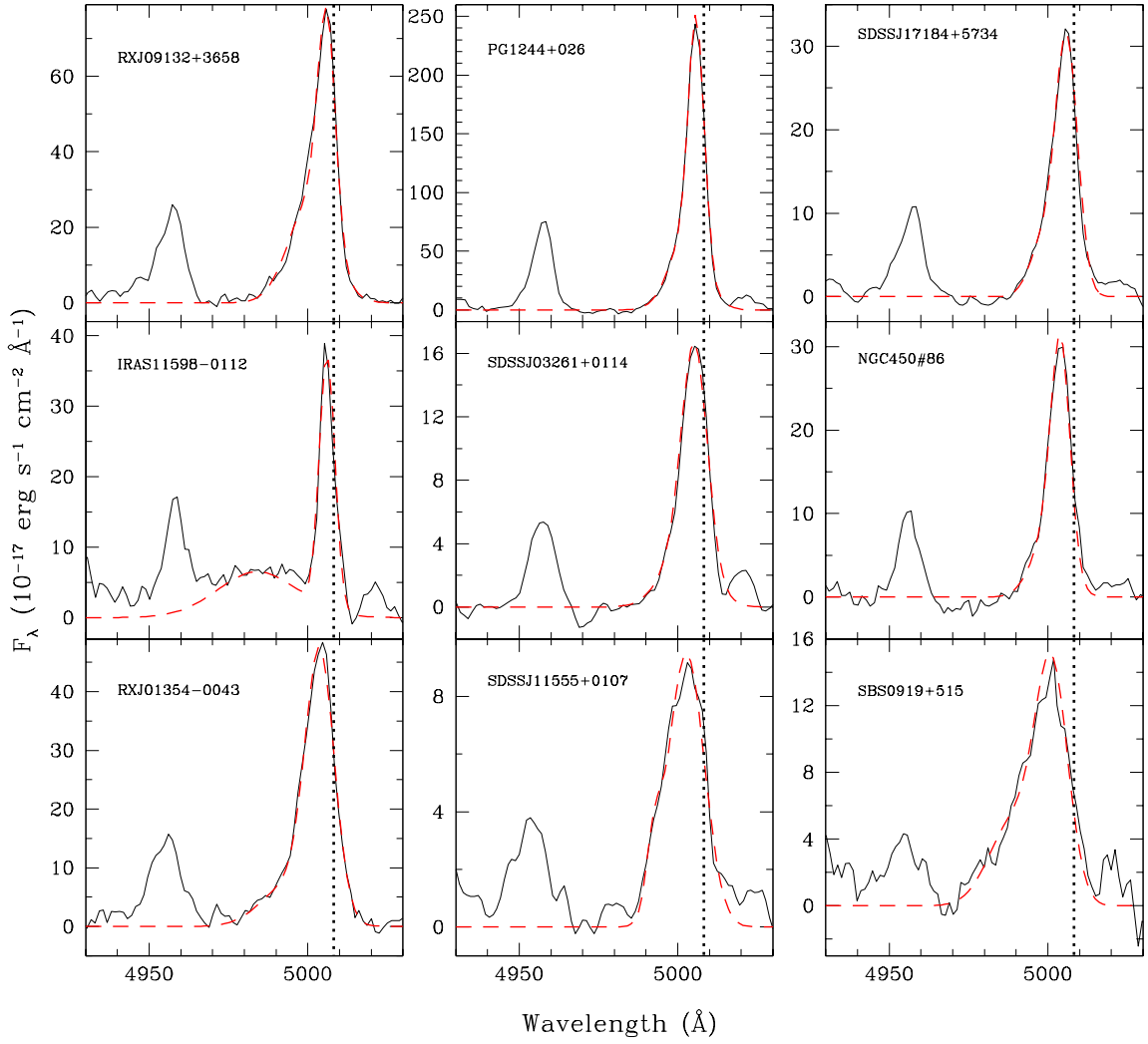


FIG. 2.— [OIII]4959,5007 emission-line region of all nine blue outliers (FeII and continuum subtracted). The expected [OIII] peak location according to [SII] is marked with the dotted line. Our two-component Gaussian fit to each [OIII]5007 emission line is overlotted using a dashed line.

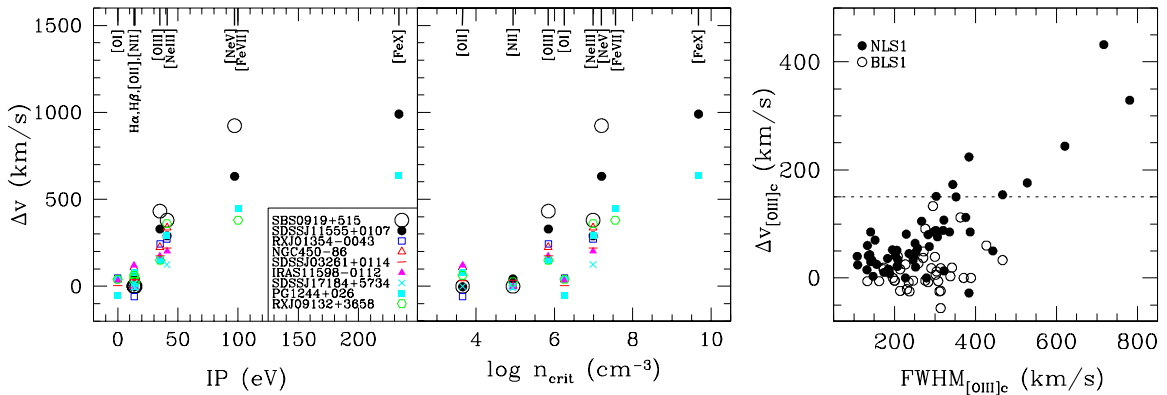


FIG. 3.— Velocity shift of individual emission lines versus the ionization potential IP and the critical density n_{crit} (left), and correlation of the [OIII] line width with the [OIII] blueshift (right).

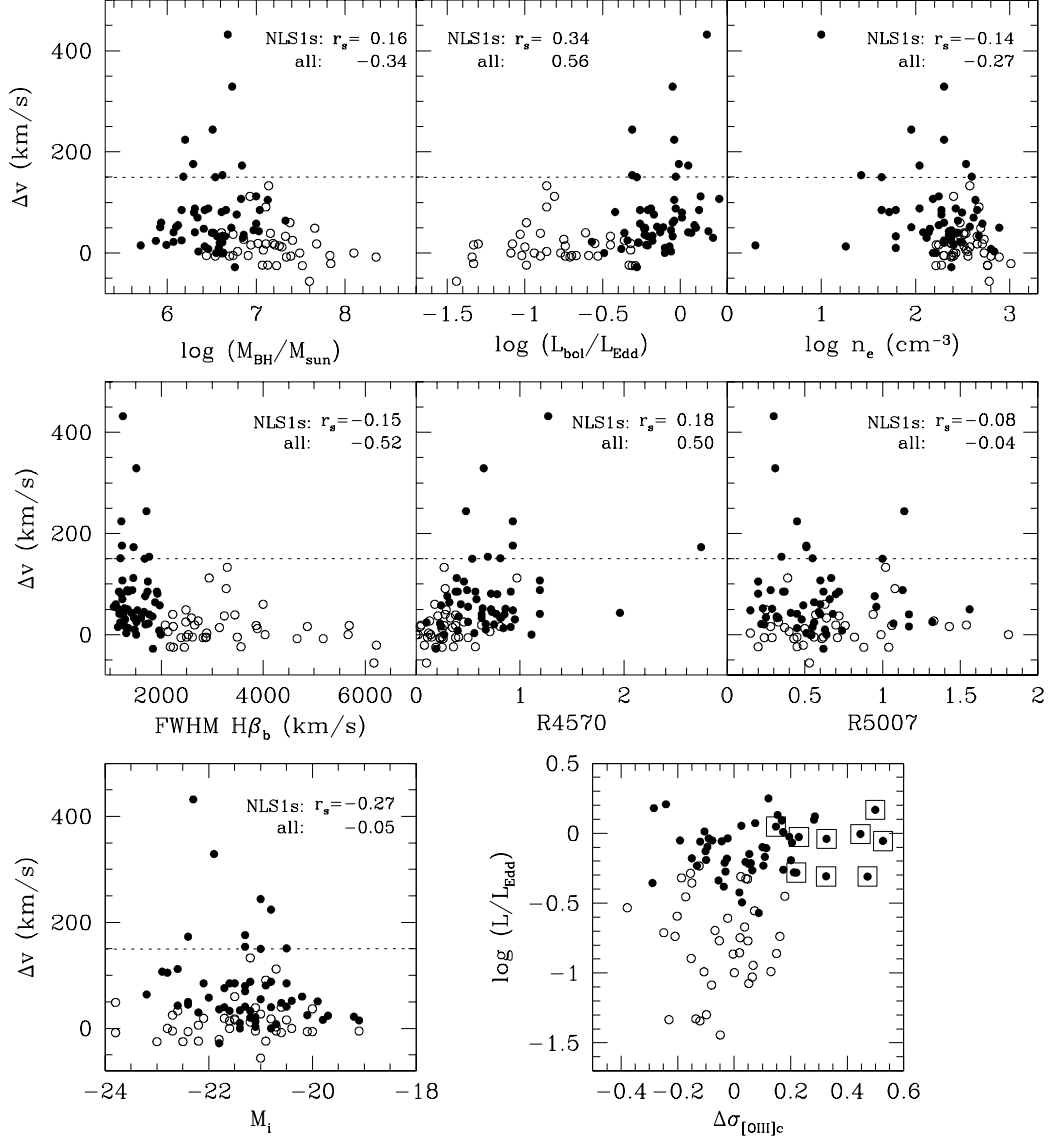


FIG. 4.— Correlation of [OIII] outflow velocity with other emission-line and AGN properties (panels 1-7). Objects above the dashed line are blue outliers. NLS1 galaxies are represented by filled circles, BLS1 galaxies by open circles. The correlation coefficient r_s shown in each panel was calculated among the NLS1 population only, or for the whole sample (marked as “all:” in the graphs). If the BLS1 galaxies are included, several correlations emerge, and the blue outliers amplify these trends. R5007 corresponds to the ratio of total [OIII] over total $H\beta$ emission, R4570 to the ratio of FeII4570 over total $H\beta$ emission. The last panel shows the galaxies’ deviation $\Delta\sigma$ (see text for definition) from the $M_{\text{BH}} - \sigma_*$ relation, in dependence of Eddington ratio. An apparent correlation does no longer exist once the blue outliers (marked with extra open squares) are removed.

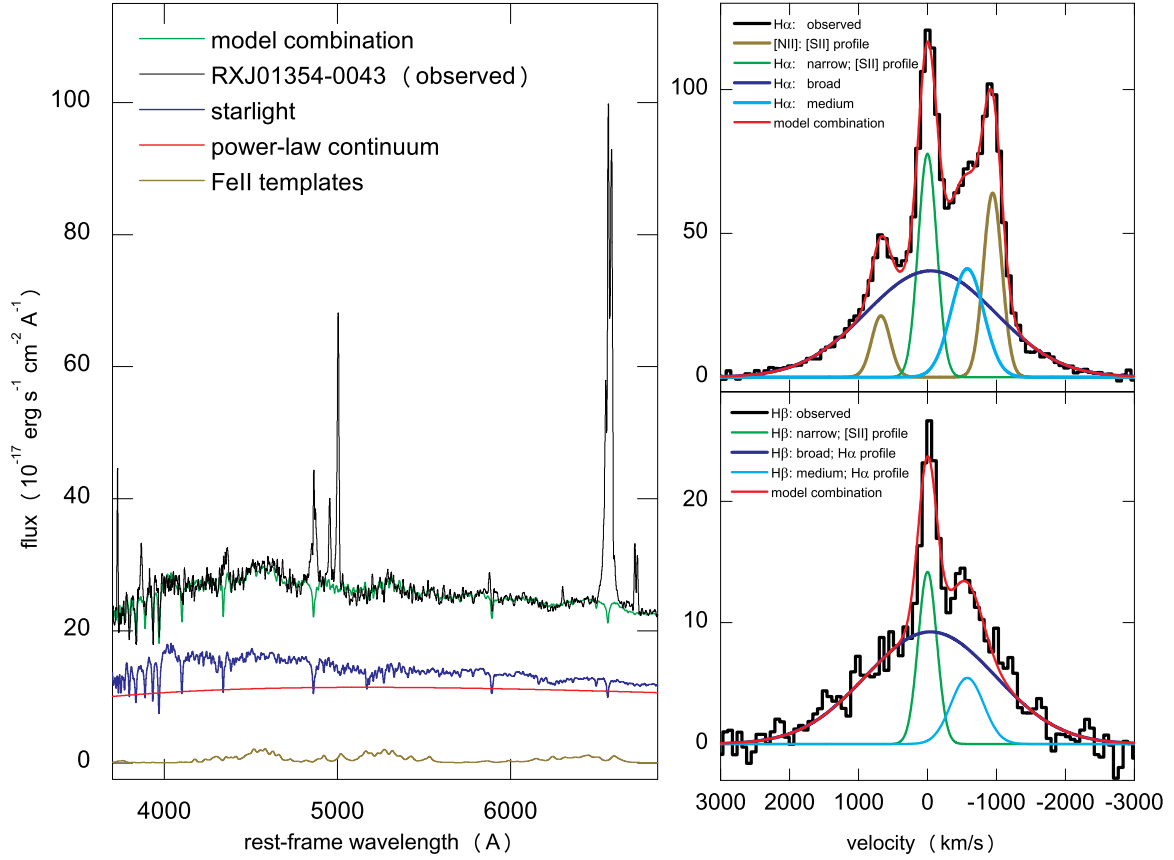


FIG. 5.— Left: SDSS spectrum of RXJ0135–0043, and component decomposition into FeII complexes, a reddened AGN powerlaw continuum, and host galaxy contribution as labeled in the figure. Strong absorption lines from the host galaxy are visible. Right: Zoom onto the H α and H β lines, showing the presence of two narrow cores of each Balmer line (green and light blue; note that in this paper, we use positive velocities to indicated blueshifts, negative values for redshifts), and a broad base (dark blue). [See the electronic edition of the *Journal* for a colour version of this figure.]